CrystEngComm

ROYAL SOCIETY OF CHEMISTRY

PAPER

View Article Online
View Journal | View Issue

Cite this: *CrystEngComm*, 2022, **24**, 7109

High-pressure, high-temperature synthesis of nanostructured polydiphenylbutadiyne confined in the 1-dimensional pores of single crystal $AlPO_4$-54†

Marco Fabbiani,[a] Sebastiano Romi,[b] Frederico Alabarse,[c] Anna Celeste,[d] Francesco Capitani,[d] Ferenc Borondics,[d] Christophe Sandt,[d] Sylvie Contreras,[e] Leszek Konczewicz,[ef] Jérôme Rouquette,[a] Mario Santoro[bg] and Julien Haines*[a]

The π-conjugated polymer polydiphenylbutadiyne was prepared at the nanoscale confined inside the 1.2 nm 1-D pores of the aluminophosphate $AlPO_4$-54. Molten 1,4-diphenyl-1,3-dibutadiyne (DPB) was inserted in the pores of $AlPO_4$-54 at pressures below 0.3 GPa as confirmed by X-ray diffraction. Heating to 190 °C under a pressure of 0.4 GPa induced polymerization of DPB in the pores. Infrared microscopy indicates full polymerization in the pores and the presence of characteristic saturated C–H defects common to other nanostructured PDPB materials exhibiting important photocatalytic properties. This nanostructured PDPB confined in the hygroscopic $AlPO_4$-54 host could be of interest for applications in gas sensing, photocatalysis and hydrogen generation.

Received 7th July 2022,
Accepted 13th September 2022

DOI: 10.1039/d2ce00938b

rsc.li/crystengcomm

Introduction

Nanoconfinement is a powerful way to modify the structure and electronic properties of π-conjugated polymers. In particular, the use of high pressure to insert and then polymerize unsaturated hydrocarbon molecules in zeolites was found to be a way to favor selected isomers due to the effects of nanoconfinement.[1–3] In the case archetypical conducting polymer polyacetylene, the *cis* or *trans* form was found to be favored depending on the form of the pores of the zeolite.[1,3] Based on theoretical calculations, this can result in isolated semiconducting or metallic polymer chains confined in an insulating host zeolite.[3] Nanoconfinement also prevents the branching of polymer chains and enabled linear polycarbonyl[2,3] to be synthesized, for example. Organic–inorganic hybrid composites of this type based on π-conjugated polymers prepared at high pressures in host zeolites may also have practical applications. In the case of polyphenylacetylene, which has potential applications in organic electronics, the composite formed by polymerization of phenylacetylene (PhA) under high-pressure, high temperature conditions in the pores of a 1.2 nm pore aluminophosphate $AlPO_4$-54 was found to exhibit selective response to certain simple molecules and may be used as a component in gas sensing devices.[4]

A substituted polydiacetylene of considerable interest is poly(1,4-diphenyl-1,3-butadiyne) or PDPB. Nanostructures of this polymer have been found to have semiconducting properties, which open the way for applications in photocatalysis, self-cleaning surfaces, hydrogen generation and solar light harvesting.[5–7] Polymerization of DPB in porous materials under high pressure could give rise to novel nanostructures based on isolated PDPB in a porous host material. Confinement may also favor certain isomers, in particular the 1,4 addition product, which has a less bulky polymer chain. In bulk DPB, previous work showed that pressures greater than 5 GPa are required to start the formation of PDPB;[8] however, mild heating at a temperature of 250 °C resulted in polymerization at a pressure of 0.86 GPa.[9]

Based on our previous work on the PPhA-based system,[4] we again selected $AlPO_4$-54 as a candidate for the host

[a] *ICGM, CNRS, Université de Montpellier, 34293 Montpellier, France. E-mail: julien.haines@umontpellier.fr*
[b] *European Laboratory for Non Linear Spectroscopy, LENS, 50019 Sesto Fiorentino, Italy*
[c] *Elettra Sincrotrone Trieste, Trieste, 34149, Italy*
[d] *Synchrotron SOLEIL, Saint Aubin – BP48, Gif sur Yvette, 91192, France*
[e] *Laboratoire Charles Coulomb, CNRS, Université de Montpellier, 34095 Montpellier, France*
[f] *Institute of High Pressure Physics, Warsaw, Poland*
[g] *Istituto Nazionale di Ottica, INO-CNR, 50019 Sesto Fiorentino, Italy*
† Electronic supplementary information (ESI) available. See DOI: https://doi.org/10.1039/d2ce00938b

material considering its large 1.2 nm diameter pores, which from a steric point of view could host PDPB. $AlPO_4$-54 is a hydrated aluminophosphate with the hexagonal Virginia Polytechnic Institute – Five VFI structure[10] (space group $P6_3$, a = 18.9678 Å and c = 8.0997 Å, $Al_{18}P_{18}O_{72}{\cdot}xH_2O$).[11] The framework of this structure is built up of PO_4 and AlO_4 tetrahedra and $AlO_4(H_2O)_2$ octahedra around 1-dimensional 1.2 nm diameter pores. This material is hygroscopic and in the as-synthesized material, the pores are filled with water molecules under ambient conditions. In the case of a nanocomposite based on VFI and PDPB, this hygroscopic character could be of interest for various applications such as gas sensing, photocatalysis and hydrogen generation. In the present paper, we have determined the pressure and temperature conditions required to insert and polymerize DPB in the VFI host to form a composite based on isolated PDPB chains in the hygroscopic porous host material.

Experimental methods

1,4-Diphenylbutadiyne (99% purity) was obtained from Sigma-Aldrich. The insertion and polymerization of DPB in the pores of VFI was investigated in two types of VFI samples: small polycrystals and large, needle-like single crystals, with linear dimensions of approximately 30 × 1 × 1 μm^3 and 200 × 25 × 25 μm^3, respectively. These materials were synthesized by an optimized sol–gel procedure followed by hydrothermal treatment from nanometric alumina and phosphoric acid or polyphosphoric acid, respectively.[11,12] Partial dehydration was performed by exposing the sample to primary vacuum at room temperature, which removes the pore water while retaining some portion of the water coordinated at the 6-fold coordinated Al in the framework.[13]

In order to perform the *in situ* high-pressure (HP), high-temperature (HT) X-ray diffraction experiments, VFI and DPB powders were mixed and loaded in a membrane diamond anvil cell (DAC, Boehler Almax, type IA diamonds, 600 μm culets), along with ruby[14,15] and SrB_4O_7:Sm^{2+} pressure gauges[16–19] in the hole of the stainless steel gasket, having a diameter and a thickness of 200 μm and 50 μm, respectively. The open DAC containing the VFI sample was placed in a vacuum chamber with Kapton windows equipped with a heater. After partial dehydration of the VFI in the vacuum chamber, the DAC was remotely closed, through the membrane, pressurized and the sample heated. The temperature was measured with a thermocouple and an extra ruby was placed on the external surface of the diamond window to check the temperature.

High pressure synchrotron powder X-ray diffraction (λ = 0.4957 Å) measurements in the heated, membrane-driven diamond anvil cell were performed with an 80 μm beam spot on the sample on the Xpress beamline equipped with a MAR345 image plate detector at the ELETTRA Sincrotrone Trieste (Trieste, Italy). The XRD images were converted to 1-D diffraction profiles using Dioptas[20] based on a calibration using NIST SRM 674b CeO_2 (a = 5.411651 Å (ref. 20)) as a standard. The sample to detector distance was determined to be 479.94 mm based on this calibration. Pressure was measured before and after every X-ray exposure using the $^7D_0$–$^5F_0$ line[19] of SrB_4O_7:Sm^{2+}. The temperature was based on the shift of the R_1 fluorescence line[18] of a ruby that was at constant pressure on the external surface of the diamond window and further checked by measurements with a K-type thermocouple on the bottom of the DAC.

Large volume, high-pressure experiments were performed in a high pressure bomb connected by a flexible capillary to a UNIPPRESS three-stage gas compressor using helium gas as a pressure transmitting medium. The pressure in the system was measured based on the variation of the resistance of a manganin coil placed in the main vessel of the compressor and kept at stable, room temperature independent of the temperature changes in the high pressure chamber. VFI and DPB powders were first mixed and placed inside a PTFE capsule with an internal volume of 0.58 cm^3 and then partially dehydrated in a glovebox entrance chamber. The capsule was placed in a glass tube under an Ar atmosphere in the glovebox. The glass tube was sealed and heated to 100 °C for 1 h to pre-melt the DPB and obtain a homogeneous mixture. The capsule was placed in a high-pressure chamber equipped with a resistive heater in order to process the sample under HP–HT conditions.

The samples obtained from the large volume synthesis and from the infrared spectroscopy experiments described below were analyzed by *ex situ* synchrotron XRD measurements on the same beamline. In the case of the single crystal recovered from the infrared experiment in the gasket, a phi-scan from −30 to 30° was performed. A Dectris Pilatus 6 M detector was used for this experiment.

Le Bail fits to obtain the unit cell parameters and Rietveld refinements were performed using the program Fullprof.[21] The quoted estimated standard deviations for the lattice parameters and the fractional atomic coordinates are those obtained directly from these refinements. Fractional atomic coordinates for the framework from previous work were used as the starting model for VFI.[11] Soft constraints were applied to the Al–O, P–O and O–O distances. An overall isotropic atomic displacement parameter (ADP) was used for all Al, P, O and C atoms as no improvement was obtained using individual ADPs. Crystal structures were displayed using the program VESTA.[22]

In situ HP–HT synchrotron infrared (IR) measurements were performed in transmission mode in the mid-IR region by using a horizontal microscope developed on the SMIS beamline (synchrotron SOLEIL) and dedicated to HP measurements in DACs. SMIS is equipped with a Thermo Fisher spectrometer (Nicolet iS50 FT-IR) modified to operate with the synchrotron radiation, which coupled with custom made Schwarzschild objectives (magnification of 15×, numerical aperture of 0.5 and working distance of 43 mm) allows a beam spot of about 30 μm diameter on the sample inside the DAC. The mid-IR spectral domain (650–8000 cm^{-1}) was investigated by using a KBr beamsplitter and a mercury

cadmium telluride (MCT) detector, and data were acquired with a resolution of 2 cm^{-1} averaging 1000 or 500 scans. The background of the empty DAC was obtained with the same resolution, averaging 200 scans, and was used for subtraction. Collected spectra were first treated by using the Omnic software. The single crystal VFI sample and the powdered DPB were placed along with a ruby as the pressure sensor in a 210 μm × 50 μm (diameter × thickness) hole in a stainless steel gasket. The cell was then subjected to primary vacuum to dehydrate the single crystal and entered into a glove box, in which the cell was closed. The DAC had 600 μm IIas type diamond culets. External resistive heating was used to heat the DAC, with the temperature measured by a K-type thermocouple. Additional measurements of recovered samples in gaskets were performed using a Continuum microscope and a Thermo Fisher Nicolet 8700 spectrometer using synchrotron radiation with a 20 μm diameter beam. The background was measured with the same beam diameter.

Two-dimensional IR hyperspectral images of the recovered sample under ambient conditions in the gasket hole were acquired with an Agilent Cary 670 spectrometer coupled to an Agilent Cary 620 microscope using a Globar as a light source. Detection was performed with a 2D 128 × 128 pixel focal plane array (FPA) detector giving a projected pixel size of 3.3 × 3.3 μm^2 with a 25× objective (NA = 0.81). The Quasar software was used to prepare the images[23,24] (**https://quasar.codes**). Details concerning the image generation are given in the ESI.†

Results and discussion

In situ and *ex situ* X-ray powder diffraction

Mixtures of VFI and DPB were investigated at pressures up to 3 GPa and temperatures up to 260 °C by *in situ* and *ex situ* synchrotron XRD in order to determine the conditions required to melt DPB and then insert the molecules in the pores of VFI without inducing phase transitions in the VFI. Based on the P–T phase diagram of DPB,[9] the liquid phase is only stable in a triangular region at pressures below 0.4 GPa and temperatures below 250 °C. The melting temperature increases from 86 °C at room pressure to approximately 250 °C at 0.4 GPa. Polymerization occurs from the liquid phase at temperatures higher than 250 °C. A large number of runs were performed with the goal of compressing the DPB–VFI mixtures at temperatures at which DPB is a liquid. In most experiments, VFI transformed at least partially to $AlPO_4$-8 with collapsed pores[25] indicating that not enough liquid DPB was present to completely fill the pores. A second limit to filling VFI was observed in experiments in which the maximum temperature was greater than 192 °C, where dense tridymite and/or berlinite phases of $AlPO_4$ were obtained. These results indicated that optimal filling conditions required the VFI to be pressurized in excess liquid DPB at temperatures below 192 °C.

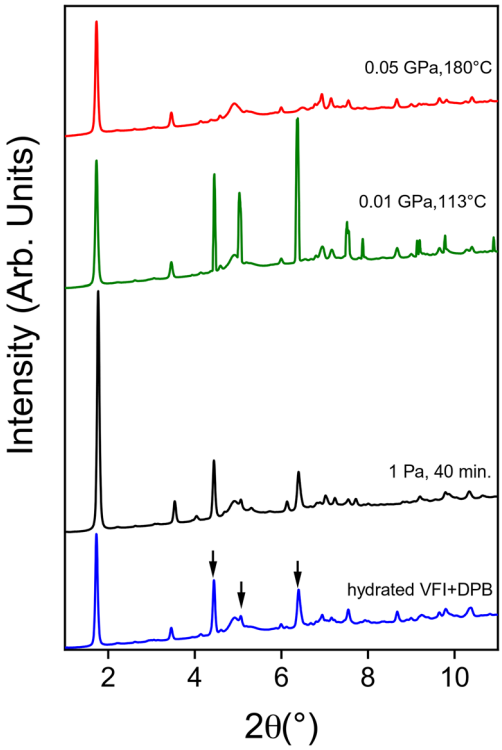

Fig. 1 X-ray powder diffraction patterns (λ = 0.4957 Å) of the VFI–DPB system during the dehydration and filling processes. Arrows indicate the strongest DPB reflections. The broad peak at close to 5° is due to the Kapton windows of the vacuum chamber.

In the following, the results of runs under these optimized conditions will be described. The result of an experiment on a DPB–VFI mixture heated to 180 °C and compressed to 0.05 GPa is shown in Fig. 1. The diamond anvil cell was left slightly open and was first exposed to a primary vacuum of 1 Pa to remove the adsorbed H_2O molecules in the pores of VFI. Due to the structural change involving the loss of H_2O and the conversion of the Al-centred octahedra to AlO_4 tetrahedra when going from the hexagonal hydrated material to the monoclinic dehydrated material, the positions and intensities of the reflections are modified as can be seen, for example, in a strong increase in the intensity of the (100) reflection of VFI below 2° in 2θ, by changes in the range between 7 and 8° in 2θ, by an important decrease in the *a* cell parameter and an increase in *c* (Table 1), as found

Table 1 Hexagonal unit cell parameters of VFI and VFI–DPB samples. The values for the *ex situ* measurement under ambient conditions on the sample processed in the large volume pressure chamber under the reported P–T conditions are given in italics

	a (Å)	*c* (Å)	*V* (Å^3)
Hydrated VFI	18.9621(7)	8.100(1)	2522.3(5)
1 Pa, 40 min.	18.5312(4)	8.330(1)	2477.4(3)
0.01 GPa, 113 °C	18.9536(9)	8.073(4)	2512(1)
0.05 GPa, 180 °C	18.9556(7)	8.167(2)	2541.4(7)
0.5 GPa, 150 °C	*18.9951(4)*	*8.133(1)*	*2541.4(3)*

previously[13] using the $P6_3$ unit cell for the hydrated material and a hexagonal subcell for the monoclinic dehydrated material. Upon reaching 0.01 GPa and heating the mixture to 113 °C, major changes occurred. The intensity of the (100) reflection decreased strongly, the *a* cell parameter increased, the *c* parameter decreased and the unit cell volume increased by 1.4%. In addition, the diffraction pattern of DPB became very spotty yielding strong sharp peaks in the resulting integrated powder pattern indicating a recrystallization of bulk DPB along with the filling of VFI due to partial melting of DPB. Upon increasing the pressure and temperature further to 0.05 GPa and 180 °C, the diffraction lines of DPB disappeared due to full melting with only the diffraction lines of dehydrated VFI remaining. The volume of VFI increased again by a further 1.2%.

A similar experiment passing by the liquid phase of DPB was performed in the large volume pressure chamber. A VFI–DPB mixture was placed in a PTFE capsule, treated under vacuum and then heated up to 100 °C to remove H_2O and melt the DPB and finally recovered at room temperature. Two phase, Rietveld refinement using synchrotron X-ray diffraction data indicated that this mixture contained 54% w/w VFI and 46% w/w DPB. The PTFE capsule was placed in the pressure chamber. The pressure was increased to 0.1 GPa and the temperature increased to 130 °C to melt the DPB. The pressure was then increased to 0.5 GPa and the temperature further increased to 150 °C. The recovered sample was studied by synchrotron powder XRD, Fig. 2. The reflections could be indexed based on the $P6_3$ space group also found for hydrated VFI. There are, however, some differences in relative intensities and the unit cell volume is slightly higher than that of hydrated VFI.

In order to perform the Rietveld refinement, a model was used beginning with the fractional atomic coordinates of the Al, P, O and structural H_2O molecules from the hydrated $P6_3$ structure in the literature.[11] Fourier difference maps were then calculated. This enabled three additional adsorbed water molecules to be located and three further peaks were identified. The adsorbed water molecules were added to the structural model as isoelectronic Ne atoms and CH residues

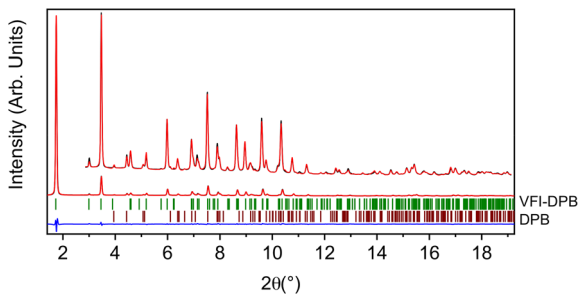

Fig. 2 Experimental (black), calculated (red) and difference (blue) profiles (λ = 0.4957 Å) for the Rietveld refinement of the DPB-filled VFI (VFI–DPB) and DPB mixture. Vertical bars indicate the calculated positions of the Bragg reflections of VFI–DPB (above) and DPB (below). A vertical zoom of the patterns from 3–19.2° is given in the inset.

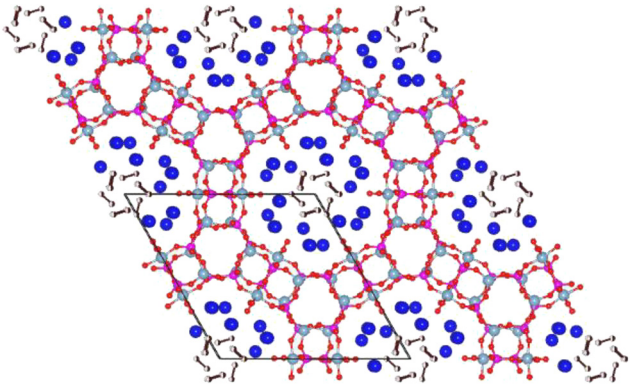

Fig. 3 Refined crystal structure of DPB-filled VFI. The pale blue, purple and red spheres represent the aluminum, phosphorus and oxygen atoms, respectively. Adsorbed H_2O molecules are represented by large blue spheres. Empty black spheres represent CH units of DPB.

of the DPB were modeled as N atoms placed on the three additional sites. A very good fit was obtained with this model (R_p = 4.0%, R_{wp} = 5.5%, R_{Bragg} = 2.1%, see Table S1 in the ESI†). As in the VFI/PPhA system,[4] the result indicated that partial rehydration occurs due to the available space around the confined polymer when the VFI/DPB composite is exposed to air in agreement with the results of infrared spectroscopy presented in the next section. The fit is already very good and thus, more detailed structural information on probably disordered DPB molecules in the pores is not accessible. The corresponding structure (Fig. 3) of VFI is characterized by an adsorbed layer of H_2O molecules in the pores and disordered DPB molecules along the pore axis. The quantitative phase analysis from the refinement indicates that the sample contains 80% w/w DPB-filled VFI and 20% w/w remaining solid DPB, thus showing that more than half of the initial quantity of DPB entered the pores of VFI. These results confirm the filling of VFI by DPB; however, powder

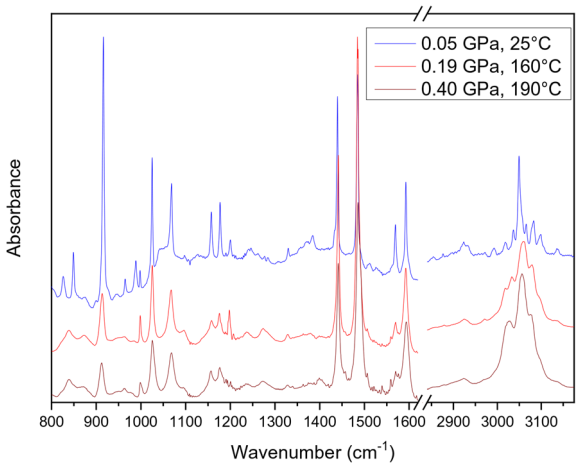

Fig. 4 *In situ* synchrotron infrared spectra of a single crystal of dehydrated VFI in DPB as functions of pressure and temperature in a diamond anvil cell. The P–T conditions correspond to solid DPB (above), liquid DPB (center) and PDPB (below).

Table 2 Principal infrared bands (cm^{-1}) of the DPB–VFI system under various P–T conditions. Detailed assignments for DPB,[28,29] PDPB[29] and VFI[11,25–27] can be found elsewhere

Solid DBP ambient	VFI + liquid DPB 0.19 GPa, 160 °C	VFI + PDPB 0.40 GPa, 190 °C	Recovered PDPB-filled VFI	Assignment
			3460vs, br	O–H
3137w	3127w	3137w		Combination
3098m	3096sh	3098sh	3099sh	C–H sp^2
3081m	3079s	3078s	3080m	C–H sp^2
3066m	3064s	3056s	3056s	C–H sp^2
3050s	3053sh			C–H sp^2
3037m	3033m	3029s	3031m	C–H sp^2
3018m	3017m	3020sh	3019m	Combination
2992m	3001sh	2995sh	3001sh	Combination
2973w	2971w	2971w		Combination
			2961sh	C–H sp^3
2933vw				Combination
	2926w	2924w	2928m	C–H sp^3
2922vw				Combination
	2879m	2878w	2877sh	C–H sp^3
2876vw				Combination
	2857w	2854w	2856m	C–H sp^3
2794vw				Combination
2681w	2680w			Combination
		Inaccessible	2213vw	Sym. C≡C
2150s	Inaccessible	Inaccessible	2151vw	Asym. C≡C
2102w	Inaccessible			
1967m	Inaccessible			Combination
1952m	Inaccessible		1952w	Combination
1896w	1894w		1896w	Combination
1881m	1876w	1879w	1879w	Combination
1824w			1819w	Combination
1806w	1797w	1797w	1803w	Combination
1752m	1749w	1748w	1749w	Combination
1739w				Combination
1670m	1668w	1666w		Combination
			1628m, br	δH–O–H
1593s	1593m	1594m	1597m	C=C phenyl
1570s	1569w	1572sh	1572w	C=C phenyl
1528w				
1512w	1507w			Overtone
		1493sh	1493sh	C=C phenyl
1485s	1485s	1487s	1487s	C=C phenyl
1440s	1441s	1441s	1442s	C=C phenyl
		1401w	1408w	
1384w	1379w	1379w		Combination
1370w				Combination
1355w		1340w	1344w	
1329w	1329w	1328w	1328w	Phenyl
1307w				
1284w	1287sh	1288sh	1290sh	Phenyl
1276w	1273w	1273w	1275w	Phenyl
			1263br	νP–O–Al
1242w	1238w	1238w	1232w	Combination
	1207vw			
1200w	1198w		1196vw, br	C–C
1177m	1176w	1176w	1176w	Phenyl
			1160vs, br	νP–O–Al
1158m	1158w	1157w	1157w	Phenyl
			1141sh	
1097w	1096w	1096w	1099w	Combination
1068m	1067m	1068m	1070m	Phenyl
1040w				
1025m	1025m	1026m	1028w	Phenyl
		1003sh		
998w	999w	999w	1000w	Phenyl

Table 2 *(continued)*

Solid DBP ambient	VFI + liquid DPB 0.19 GPa, 160 °C	VFI + PDPB 0.40 GPa, 190 °C	Recovered PDPB-filled VFI	Assignment
987w	984w	979sh		Phenyl
964w	963w	963w	966w	Phenyl
945w	948sh	948sh	951w	
927sh				
916m	913m	912w	915m	Phenyl CH bending
899w			889w	
877w	873w	871w	877w	
848w	839w	839w	841w	Phenyl
826w	823w	821sh	822w	
758vs	752vs	753vs	750vs	Phenyl
696m	697sh	694vs		Phenyl
688s	688vs			Phenyl
670m	670m	668sh		

XRD is not the most appropriate technique to study the polymerization of DPB in the pores of VFI, as we know that the DPB entered the pores, but we do not have any direct information on its state: monomer or polymer. Complementary spectroscopic techniques are thus necessary to obtain such information on the state of DPB in the pores.

In situ and *ex situ* infrared spectroscopy

The polymerization of DPB in single crystals of VFI was investigated by IR spectroscopy. VFI single crystals were surrounded by DPB powder and treated under primary vacuum to remove adsorbed water as in the XRD studies. This was confirmed by the disappearance of the H_2O stretching and bending bands in the IR spectrum. The mixture was then heated under pressure in a diamond anvil cell, Fig. 4. Note that the two-phonon absorption of the diamonds from the DAC masked the 2100–2150 cm^{-1} region, in which the C≡C stretch of DPB is found. Apart from the weak contribution of dehydrated VFI corresponding to a very broad band between 1050 and 1300 cm^{-1} due to P–O–Al stretching,[11,25–27] the other modes are due to DPB,[28] principally dominated by the bulk DPB around the VFI single crystal. Based on the absence of changes to the IR spectrum apart from minor shifts in wavenumber, the DPB remained solid up to 140 °C and 0.2 GPa. Many changes in the spectrum occurred at 160 °C and 0.19 GPa, where the majority of bands broaden significantly and with the region between 800 and 1000 cm^{-1} being particularly affected, Table 2. Some bands disappear and a new band is observed at 837 cm^{-1}. The most intense band near 916 cm^{-1} corresponding to the phenyl C–H bending decreases strongly, but the other principal modes of the phenyl group are less affected. This is in agreement with melting of DPB as described in previous work.[29] At 190 °C and 0.40 GPa, the principal C–H stretching vibrations between 3000 and 3100 cm^{-1} broaden further. As in previous studies, the sharp band of the C–C stretch initially at 1200 cm^{-1} in the solid disappears.[29] This band corresponds to a C–C stretch in the butadiyne group and its disappearance is a clear sign of polymerization. A weak band also appears close to 1400 cm^{-1} as in previous work.[29]

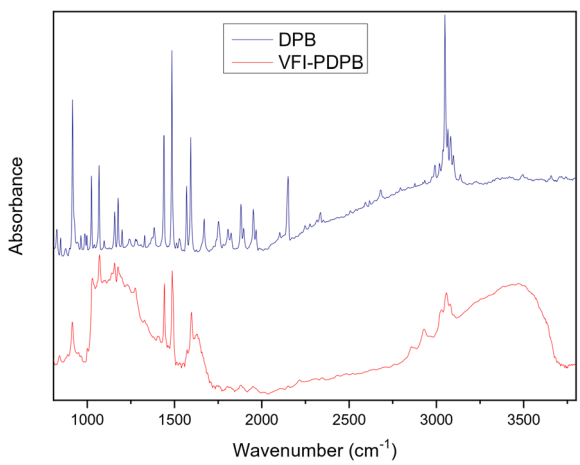

Fig. 5 Synchrotron infrared spectra of the solid DPB monomer (above) and the recovered, rehydrated single crystal of VFI filled with PDPB after heating at 190 °C at 0.4 GPa (below).

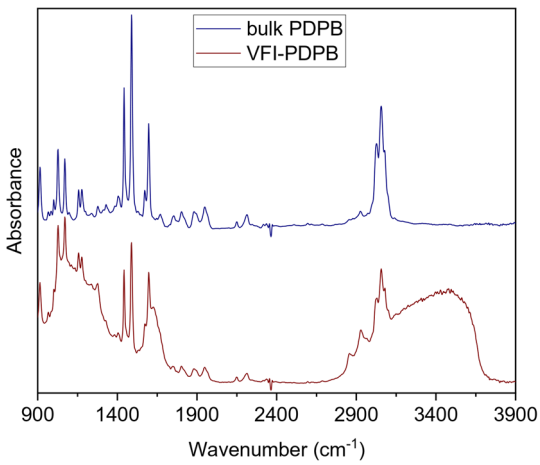

Fig. 6 Selected infrared spectra from FPA imaging of the gasket containing the recovered, rehydrated single crystal of VFI filled with PDPB (brown) and bulk PDPB (blue) after heating at 190 °C at 0.4 GPa.

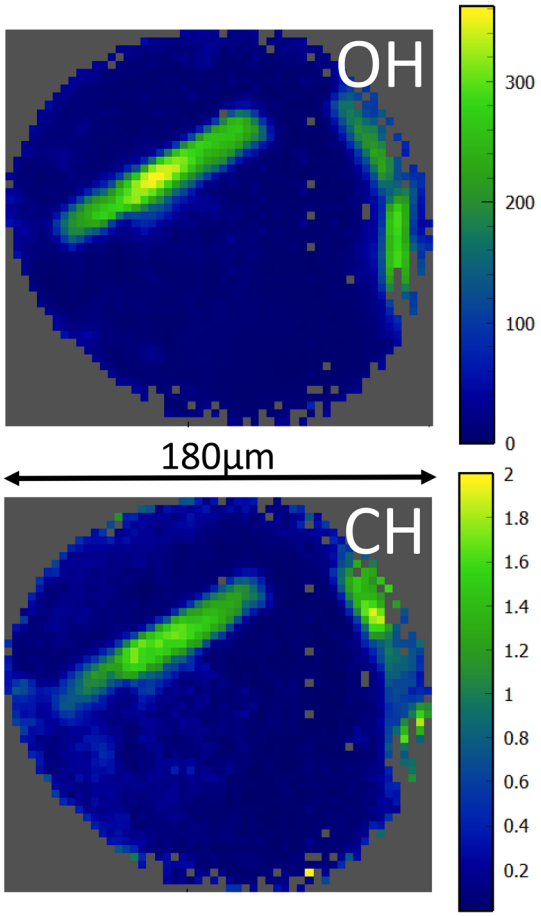

Fig. 7 Infrared spectral FPA imaging in the O–H stretching 3130–3700 cm^{-1} (above) and in the 2940–2960 cm^{-1} saturated C–H stretching (below) ranges of the spectrum of the gasket (hole diameter of 180 μm) containing the recovered, rehydrated single crystal of VFI filled with PDPB and bulk PDPB after heating at 190 °C at 0.4 GPa. The colors represent the intensity scale from weak (blue) to strong (yellow). Two fragments of a second single crystal are present on the right at the edge of the gasket hole.

Additional experiments were performed on further samples at temperatures up to 250 °C and the same spectrum was observed for the polymer. However, as found by XRD, VFI starts to transform to nonporous forms of $AlPO_4$.

Recovered, rehydrated samples were investigated using an infrared microscope with a smaller beam spot of 20 μm instead of 30 μm for the *in situ* experiment in the diamond anvil cell. The resulting higher spatial resolution allowed the PDPB in single crystal VFI to be studied more selectively. In addition, as the DAC masked the 2100–2150 cm^{-1} region, in which the C≡C stretch of DPB is found, these vibrations can now be observed directly in the recovered sample in the gasket outside the DAC, Fig. 5. In contrast to the *in situ* measurements on dehydrated VFI, broad bands due to OH stretching and bending are observed at 3460 and 1628 cm^{-1}, respectively, indicating that the VFI single crystal had rehydrated[4] as a consequence of exposure to air. The broad VFI framework P–O–Al stretching vibrations at 1263 and 1160 cm^{-1} are clearly evident in the spectrum of the single crystal. In the VFI crystal, the antisymmetric C≡C stretching band at 2150 cm^{-1} has almost disappeared in the confined PDPB polymer as compared to solid DPB indicating that the monomer is essentially entirely consumed in the polymerization reaction. In addition, a very weak peak at 2213 cm^{-1}, corresponding to the Raman-active symmetric C≡C stretching band of the DPB monomer,[28] is observed. This indicates that the center of symmetry that was present in the DPB monomer is lost, possibly due to the formation of cyclic structures of the polyacene type in the polymer.[29] Additionally, bands are observed at 2928, 2877 and 2856 cm^{-1} close to where sharper combination bands are observed for solid monomeric DPB. Such bands close to saturated C–H stretching mode frequencies are characteristic of defects (possibly isobutyl end-groups)[30] in polymeric DPB. In an infrared 2D imaging of the gasket hole, Fig. 6 and 7, it can also be seen that the intensities of these saturated C–H vibrations are correlated to the intensities of the H_2O stretching and bending vibration and the P–O stretching vibrations of the crystal and are much stronger in the crystal as compared to the surrounding bulk DPB polymer. It can thus be concluded that nanoconfinement favors such saturated C–H defects. The strong intensity of these C–H vibrations is similar to what is observed in other nanostructured PDPB materials,[5] which exhibit interesting photocatalytic properties.

The recovered IR samples were also studied by synchrotron single crystal XRD. The crystal quality was not good enough to perform a structure refinement due to a certain degree of degradation due to filling and processing under high pressure–high temperature conditions. A large number of X-ray diffraction spots could be clearly observed and they were readily indexed based on the $P6_3$ VFI structure. This indicates that the host material has lower crystal quality after processing, but retains its porous structure. This could be due to strain induced by the processing conditions or simply induced by the presence of the polymer in the pores. If the latter is the case, this is a sign of interactions between the host and the polymer guest, which could be expected to modify its electrical and optical properties.

Conclusions

Diphenylbutadiyne was melted and then inserted in the porous aluminophosphate VFI at modest pressures of less than 0.3 GPa and temperatures of 110–160 °C depending on the pressure. Upon increasing the temperature to 190 °C at 0.4 GPa, polymerization of DPB was found to occur. Volume changes and Rietveld refinements using X-ray diffraction data confirmed the insertion of DPB in VFI. The polymerization of DPB in the pores of VFI was clearly demonstrated by infrared microscopy. The precise and reproducible determination of the relatively modest pressures and temperatures of 0.4 GPa

and 190 °C for the filling and polymerization of DPB in VFI indicates that these conditions correspond to those routinely used in industrial large-volume high pressure devices thus opening the way to scale up the synthesis of this material. The nanoconfined PDPB polymer exhibits characteristic saturated C–H vibrations, which have been observed for other nanostructured PDPB materials[5] exhibiting interesting photocatalytic properties. Nanocomposites obtained from the insertion of PDPB in the hygroscopic host VFI could be of interest for photocatalytic hydrogen generation with a continuous source of water or as a component in gas sensors.

Author contributions

Mario Santoro and Julien Haines (conceptualization); Julien Haines (writing – original draft); Mario Santoro, Francesco Capitani and Julien Haines (writing – review & editing); Marco Fabbiani, Sebastiano Romi, Frederico Alabarse, Francesco Capitani, Ferenc Borondics, Christophe Sandt, Jérôme Rouquette, Mario Santoro and Julien Haines (data curation and formal analysis); Marco Fabbiani, Sebastiano Romi, Frederico Alabarse, Anna Celeste, Francesco Capitani, Ferenc Borondics, Christophe Sandt, Sylvie Contreras, Leszek Konczewicz, Jérôme Rouquette, Mario Santoro and Julien Haines (investigation and methodology); and Mario Santoro and Julien Haines (supervision and resources).

Conflicts of interest

There are no conflicts of interest to declare.

Acknowledgements

The synchrotron X-ray diffraction experiments were performed at the Xpress beamline from Elettra Sincrotrone Trieste (proposal number: 20205095). The synchrotron infrared experiments were performed at the SMIS beamline from Synchrotron SOLEIL (proposal number: 20191393). MS acknowledges the "Fondazione Cassa di Risparmio di Firenze" supporting his research at the INO-CNR through the SALUS grant.

References

1 D. Scelta, M. Ceppatelli, M. Santoro, R. Bini, F. A. Gorelli, A. Perucchi, M. Mezouar, A. van der Lee and J. Haines, *Chem. Mater.*, 2014, **26**, 2249–2255.
2 M. Santoro, K. Dziubek, D. Scelta, M. Ceppatelli, F. A. Gorelli, R. Bini, J. M. Thibaud, F. Di Renzo, O. Cambon, J. Rouquette, P. Hermet, A. van der Lee and J. Haines, *Chem. Mater.*, 2015, **27**, 6486–6489.
3 M. Santoro, D. Scelta, K. Dziubek, M. Ceppatelli, F. A. Gorelli, R. Bini, G. Garbarino, J. M. Thibaud, F. Di Renzo, O. Cambon, P. Hermet, J. Rouquette, A. van der Lee and J. Haines, *Chem. Mater.*, 2016, **28**, 4065–4071.
4 F. G. Alabarse, M. Polisi, M. Fabbiani, S. Quartieri, R. Arletti, B. Joseph, F. Capitani, S. Contreras, L. Konczewicz, J. Rouquette, B. Alonso, F. Di Renzo, G. Zambotti, M. Bau, M. Ferrari, V. Ferrari, A. Ponzoni, M. Santoro and J. Haines, *ACS Appl. Mater. Interfaces*, 2021, **13**, 27237–27244.
5 S. Ghosh, N. A. Kouame, L. Ramos, S. Remita, A. Dazzi, A. Deniset-Besseau, P. Beaunier, F. Goubard, P. H. Aubert and H. Remita, *Nat. Mater.*, 2015, **14**, 505–511.
6 S. Sardar, P. Kar, H. Remita, B. Liu, P. Lemmens, S. K. Pal and S. Ghosh, *Sci. Rep.*, 2015, **5**, 17313.
7 Y. H. Wang, Y. X. Deng, L. G. Fan, Y. Zhao, B. Shen, D. Wu, Y. Zhou, C. C. Dong, M. Y. Xing and J. L. Zhang, *RSC Adv.*, 2017, **7**, 24064–24069.
8 W. S. Tang and T. A. Strobel, *ACS Appl. Polym. Mater.*, 2019, **1**, 3286–3294.
9 Y. Kojima, T. Matsuoka and H. Takahashi, *J. Mater. Sci. Lett.*, 1996, **15**, 539–541.
10 L. B. Mccusker, C. Baerlocher, E. Jahn and M. Bulow, *Zeolites*, 1991, **11**, 308–313.
11 F. G. Alabarse, J. Haines, O. Cambon, C. Levelut, D. Bourgogne, A. Haidoux, D. Granier and B. Coasne, *Phys. Rev. Lett.*, 2012, **109**, 035701.
12 F. G. Alabarse, G. Silly, A. Haidoux, C. Levelut, D. Bourgogne, A. M. Flank, P. Lagarde, A. S. Pereira, J. L. Bantignies, O. Cambon and J. Haines, *J. Phys. Chem. C*, 2014, **118**, 3651–3663.
13 M. Fabbiani, M. Polisi, B. Fraisse, R. Arletti, M. Santoro, F. Alabarse and J. Haines, *Solid State Sci.*, 2020, **108**, 106378.
14 G. Shen, Y. Wang, A. Dewaele, C. Wu, D. E. Fratanduono, J. Eggert, S. Klotz, K. F. Dziubek, P. Loubeyre, O. V. Fat'yanov, P. D. Asimow, T. Mashimo, R. M. M. Wentzcovitch, J. Bass, Y. Bi, D. He, K. V. Khishchenko, K. Leinenweber, B. Li, T. Sakai, T. Tsuchiya, K. Shimizu, D. Yamazaki, M. Mezouar and I. T. Grp, *High Pressure Res.*, 2020, **40**, 299–314.
15 H. K. Mao, J. Xu and P. M. Bell, *J. Geophys. Res.: Solid Earth*, 1986, **91**, 4673–4676.
16 A. Lacam and C. Chateau, *J. Appl. Phys.*, 1989, **66**, 366–372.
17 F. Datchi, R. LeToullec and P. Loubeyre, *J. Appl. Phys.*, 1997, **81**, 3333–3339.
18 F. Datchi, A. Dewaele, P. Loubeyre, R. Letoullec, Y. Le Godec and B. Canny, *High Pressure Res.*, 2007, **27**, 447–463.
19 S. V. Rashchenko, A. Kurnosov, L. Dubrovinsky and K. D. Litasov, *J. Appl. Phys.*, 2015, **117**, 145902.
20 C. Prescher and V. B. Prakapenka, *High Pressure Res.*, 2015, **35**, 223–230.
21 J. Rodriguez-Carvajal, *Appl. Crystallogr.*, 2001, 30–36.
22 K. Momma and F. Izumi, *J. Appl. Crystallogr.*, 2011, **44**, 1272–1276.
23 M. Toplak, G. Birarda, S. Read, C. Sandt, S. M. Rosendahl, L. Vaccari, J. Demšar and F. Borondics, *Synchrotron Radiat. News*, 2017, **30**, 40–45.
24 M. Toplak, S. T. Read, C. Sandt and F. Borondics, *Cells*, 2021, **10**, 2300.

25 F. G. Alabarse, J. B. Brubach, P. Roy, A. Haidoux, C. Levelut, J. L. Bantignies, O. Cambon and J. Haines, *J. Phys. Chem. C*, 2015, **119**, 7771–7779.
26 A. J. Holmes, S. J. Kirkby, G. A. Ozin and D. Young, *J. Phys. Chem.*, 1994, **98**, 4677–4682.
27 N. Venkatathri, *Bull. Mater. Sci.*, 2003, **26**, 279–281.
28 G. Baranovic, L. Colombo, K. Furic, J. R. Durig, J. F. Sullivan and J. Mink, *J. Mol. Struct.*, 1986, **144**, 53–69.
29 B. Zimmermann and G. Baranovic, *Vib. Spectrosc.*, 2006, **41**, 126–135.
30 A. A. Berlin, M. I. Cherkashin, M. G. Chauser and R. R. Shifrina, *Polym. Sci.*, 1967, **9**, 2510–2517.